A Two-Telescope Receiver Design for Deep Space Optical Communications

K. Shaik
Communications Systems Research Section

A two-telescope system for a deep space optical communication receiver is proposed. To substantially improve the overall receiver efficiency, the design reserves the large telescope for signal-detection purposes only. A small diffraction-limited telescope is introduced to accomplish the task of navigational tracking.

I. Introduction

A 10-m hexagonally segmented Cassegrain optical telescope has been proposed for use as an Earth-vicinity receiver for laser communications from planetary spacecraft [1–3]. Such a reception station on the ground may provide, for example, a channel capacity of 5 Mbits/sec for a 0.3-m-diameter transmitter at Mars. Even though the first reception station will be ground based, the goal is to develop and demonstrate technology which can be used to put a telescope into Earth orbit to avoid the deleterious effects of the atmosphere on optical communications. The technology has to be economical enough to allow replication for either a ground- or a space-based network.

The present design requires a demonstration of direct detection of optical signals for typical data rates from planetary spacecraft in the presence of considerable solar background interference, and also the ability to acquire and track spacecraft signals relative to the stellar background by means of a single 10-m telescope. Since the two functions have somewhat different requirements, the necessary compromises are likely to make the system less efficient. This difficulty can be avoided by including a well-corrected second telescope that is roughly one meter in diameter at a relatively small cost to the system, to accomplish the acquisition and navigational tracking of spacecraft, which leaves the larger telescope for signal-detection purposes only. The following sections discuss the motivation for and the design aspects of a two-telescope optical reception station.

Note that the introduction of a small, well-corrected telescope cannot contend or compete with the signal-detection capabilities of the large telescope. For short signal pulses, the small telescope will become photon starved for most ranges of interest. It is only when the integration times can be long, as in the case of navigational tracking, that the small telescope becomes a useful tool by providing a good signal-to-noise-ratio (SNR) for daytime observations. The introduction of a small telescope also provides an opportunity to optimize the design of the large telescope for communications. The following discussion focuses only on the navigational tracking of the spacecraft and describes derivative benefits for the receiver system if a two-telescope approach is adopted.

II. System Design with Two Telescopes

A. Motivation

The cost of a telescope depends heavily on the size and the surface accuracy of the primary mirror. A large collector area (primary) is needed to ensure that there are enough photons per signal pulse for the detector. The image quality, however, can be sacrificed by accepting a high-surface-tolerance primary. The present design and cost analysis permit a primary with a root-mean-square tolerance of about four wavelengths in the visible range. Also, the design envisions a fast primary ($f/0.5$), and no active or adaptive figure-control mechanism for the correction of gravity sag and other tilt errors. Such decisions considerably reduce the cost of a complete system; however, the expected spot size at the focus becomes quite large. Calculations show that the contribution to the blur circle by the mirror surface roughness alone will have a half-width, half-maximum (HWHM) angle of about 50 μrad for a point source. A further deterioration of similar magnitude is expected due to the gravity sag, atmospheric seeing, and other errors, making the eventual system HWHM angle for the blur circle about 100 μrad.

Radiant intensity (watt/steradian) at the focus is proportional to A_c/ϕ^2, where A_c is the area of collection for the mirror and ϕ is the blur circle HWHM angle for a point source. The HWHM blur angle for a diffraction-limited 1-m telescope is largely determined by atmospheric conditions. Hence, everything else being the same, the radiant intensity for a diffraction-limited 1-m telescope with a nominal $\phi \simeq 3$ μrad will be about 10 times higher than that for a 10-m telescope with $\phi \simeq 100$ μrad. Under adverse atmospheric conditions (seeing $\phi \simeq 10$ μrad), which may occur less than 10 percent of the time during the midmornings and the late afternoons at well-chosen sites, the smaller telescope can do no worse than the larger telescope. Such extreme conditions, however, can be avoided by scheduling the acquisition and tracking events at other times.

For the large, one-telescope system, when the task of navigational tracking of the spacecraft coordinates at the tracking detector is to be performed simultaneously with the gathering of signal photons at the communications detector, only a small fraction of the collected light can be directed to the tracking detector without jeopardizing the prime function of the telescope. Assuming 10 percent of the light for the one-telescope system going to the tracking detector, the radiant intensity for the small telescope, which is dedicated to navigational tracking only, can be 100 times higher than that of the large telescope. However, calculations in Section B of this article ignore this fact and assume that all the light collected by the large telescope is available for navigational tracking.

Use of a two-telescope arrangement provides a number of opportunities to optimize the design of each of the telescopes for its designated function. Some of these refinements, which may substantially improve the system sensitivity, are discussed in the following paragraphs.

The less efficient broadband optical coating required to image starfields for acquisition and tracking for the 10-m telescope can be discarded in favor of a highly efficient narrowband optical coating specific to the signal wavelength. The reflectance per surface can go up from about 0.75 to 0.98, resulting in (1) an increase of more than 1 dB per surface in the available radiant intensity at the signal detector, and (2) a substantial decrease in out-of-band background noise, which may help simplify the post-tertiary optical design.

The stray-light rejection capabilities for the system can be much higher. Since the small telescope, with its broad field of view (FOV), is now used for blind pointing, acquisition, and tracking, the FOV of the large telescope can be decreased to limit stray light, albeit at the expense of introducing some complexity by requiring a mechanism to transfer accurate position coordinates from the small to the large telescope.

Indeed, some form of restriction on the telescope passband or on the FOV, or both, may be necessary to protect the post-tertiary optics for a one-telescope receiver. Under certain conditions, the collected energy for the 10-m telescope for daytime observations can be several watts. Special schemes may have to be devised to protect the detectors and to dissipate the heat generated.

Post-tertiary optics are further simplified as there is no need for a removable beam deflector with its random mechanical placement errors to direct the beam to the tracking detector, when intermittent acquisition and tracking updates are required. The case of a permanent beam splitter for continuous tracking has already been discussed above.

B. Telescope Performance for Navigational Tracking

The baseline parameter values for deep space optical communications envisioned for Moon-Earth, Mars-Earth, Saturn-Earth, and the Thousand Astronomical Units (TAU) missions are given respectively in columns A, B, C, and D of Table 1. Using the parameter values given in Table 1, the received signal flux and the corresponding number of photoelectrons per second generated at the

detector (as well as a number of other relevant quantities) can be calculated by the computer program [4]. Data from this program are obtained for the typical link profiles described in Table 1, which are then used in the SNR formula developed below to calculate expected SNR for the telescopes in question in the presence of typical daytime and nighttime background noise.

1. SNR calculation. If n_s is the total number of signal photoelectrons per pixel at the detector, and n_b, n_{th}, n_d, and n_r represent sky background, thermal, dark-current, and readout noise photoelectrons per image spot size of a point source respectively, then the SNR is defined as

$$\text{SNR} = \frac{n_s}{[n_s + n_b + n_{th} + n_d + n_r]^{1/2}} \tag{1}$$

For observations in the visible spectral range, the noise contribution from the thermal and the dark-current noise is very small compared to the readout and the sky background noise, and will be ignored. Define the following variables:

λ = signal wavelength, nm

t = integration time, sec

η_a = Earth-atmosphere transmission efficiency

η_d = detector quantum efficiency

η_r = receiver optics efficiency

$\delta\lambda$ = source-laser bandwidth, nm

$\Delta\lambda$ = filter bandwidth centered about λ and $\delta\lambda \subseteq \Delta\lambda$, nm

f_L = signal-laser spectral flux, W/(m$^2\cdot$ nm)

A_s = noise-equivalent sky area, sr

F_s = sky-background spectral flux per solid angle, W/(m$^2\cdot$ nm $\cdot$ sr)

N = average number of photons/joule about wavelength λ

Neglecting n_{th} and n_d, and expressing the signal and the noise photocounts in terms of the variables defined above, Eq. (1) can be rewritten as

$$\text{SNR} = \frac{K f_L \delta\lambda}{[K(f_L\delta\lambda + A_s F_s \Delta\lambda) + n_r]^{1/2}} \tag{2a}$$

where A_c is the primary collector area as defined earlier, and $K = N\eta_d\eta_r\eta_a A_c t$.

Photoelectron counts per second per pixel due to the readout noise are about seven counts for a typical charge-coupled device detector. Allowing for a 50-msec integration time and a 4-pixel image size for a point source, the expected number of photoelectrons from the readout noise is found to be about 1.5 photoelectrons per integration time. Using nighttime sky background radiance given in Table 1, the corresponding number of photoelectrons for the small telescope is found to be 0.2 per 50-msec. The number of photoelectrons due to the sky background collected by the small telescope during the daytime and by the large telescope during the daytime as well as the nighttime is very large compared to all other noise sources discussed above. Therefore, for the large telescope at all times and for the small telescope during the daytime, the above equation can be further reduced to

$$\text{SNR} = \frac{K^{1/2} f_L \delta\lambda}{[f_L\delta\lambda + A_s F_s \Delta\lambda]^{1/2}} \tag{2b}$$

Determination of the effective noise area, A_s, that contributes to sky background noise is a difficult problem. It has been shown that $A_s = 2.28\pi\phi^2$ is a good approximation as long as the pixel size is less than the blur radius (ϕ in radians), and a two-dimensional Gaussian point-spread function is assumed [5–7]. This expression for the noise-equivalent area will be used to calculate specific results below.

The resonant frequency of the telescope structure, in the absence of active controls and involved post-processing of signals, determines the longest integration time. The maximum resonant frequency for the 10-m telescope structure, which may also house the tracking telescope, is expected to be about 5 Hz. Using a factor of four for safety, an integration time of 50 msec (20 Hz) can be used. Further improvement in the SNR is possible if some shuttering scheme is devised to prevent background light from reaching the detector when the signal pulse is not expected. The length of time which the detector can remain shuttered can be a large fraction of 50 msec, as the pulsewidth is likely to be much smaller ($\sim$ 10 ns) than the dead time between pulses ($\sim$ 100 μsec). However, no such shuttering scheme is assumed in the following examples.

An optical communications link program in [4] is used to calculate the expected signal power and the corresponding photoelectrons generated at the detector for the link profiles given in Table 1 for both the 1-m and the

10-m telescopes. These results are then used in conjunction with Eqs. (2a) and (2b) above to obtain SNR estimates for both the daytime and the nighttime sky-background radiances. In the case of nighttime calculations for the Moon-Earth, Mars-Earth, and the Saturn-Earth links, the presence of the Moon, Mars, and Saturn, respectively, in the background is assumed. A number of additional calculations using the TAU link profile for ranges between 50 and 1000 AU was also made.

The results for the nighttime and the daytime performance of the two telescopes are summarized in Figs. 1 and 2. In these figures, links A, B, and C assume the presence of the Moon, Mars, and Saturn, respectively, in the receiver field of view. Links D_1, D_2, D_3, and D_4 represent link-profile D in Table 1 with 50, 100, 500, and 1000 AU range, respectively. The SNR for the 1-m telescope for link profiles A through C for both the daytime and the nighttime observations remains higher than unity. Calculations with the TAU profile for the 1-m telescope were made only up to a range of 500 AU, where the signal photoelectrons begin to be comparable to the threshold of detection. In all cases except the daytime result at 500 AU, the SNR is found to be better than unity for the 1-m telescope. For the 10-m telescope, the nighttime SNR is higher than with the 1-m telescope for all link profiles considered. The daytime SNR for the Earth-Saturn and the TAU links, however, falls short of unity. Note that use of the same expression for A_s and the assumption that the entire signal power is focused on the tracking detector for the 10-m telescope may not be accurate, thereby overestimating the SNR for the larger telescope.

2. Navigational tracking and star magnitudes. To gain a sense of the magnitude of a star that may be visible to the telescope for navigation, Eq. (2b) may be expressed, in terms of star magnitudes, as follows:

$$m = -2.5 \log \left[\frac{(\mathrm{SNR})^2}{2Kn} \left\{ 1 + \left(1 + \frac{4KNF_sA_s}{(\mathrm{SNR})^2} \right)^{1/2} \right\} \right] \tag{3}$$

where m is the visual magnitude of a star and $n = 10^8$ photons/(sec·m^2 · nm) is the canonical value at the top of the atmosphere for a zero-magnitude A0 star at 550 nm. Note that the passband for both the navigational star and the background noise is limited by $\Delta\lambda = 200$ nm. This passband essentially represents the width of a V-filter, which is designed to cover the visible spectral range, and is widely used for star-tracking purposes. For SNR = 1, the above equation can be simplified to give

$$m = -2.5 \log \left[\frac{1}{2Kn} \left\{ 1 + (1 + 4KNF_sA_s)^{1/2} \right\} \right] \tag{4}$$

For the typical parameter values pertaining to the tracking telescope and the communication channels given in Table 1, a star brighter than magnitude 13 will be visible to the 1-m tracking telescope with an SNR of unity before the threshold of detection is reached for nighttime observation. The corresponding number for the 10-m telescope is found to be magnitude 18. During the daytime, the small telescope can see a star of magnitude 10 or brighter with an SNR of unity, which is better than the performance of the large telescope with a large blur radius by one visual magnitude.

C. Other Design Aspects

The size of the proposed secondary for the 10-m telescope is 1.1 m. The 1-m acquisition and tracking telescope can fit nicely on top of the secondary, but well inside the proposed sunshade for the large telescope to use it as protection against direct sunlight. This will make for a compact system. The two telescopes can be mounted rigidly with respect to each other and aligned, making the problem of angle transfer relatively simple.

It may also be possible to use the 1-m telescope as the uplink transmitter by including an uplink laser with steering mirrors for the point-ahead.

III. Conclusion

In a two-telescope design for a deep space optical communication reception station, each of the two telescopes can be optimized for its appointed function. This configuration provides a better daytime SNR and an adequate nighttime SNR for most missions within the solar system. However, it fails to perform well for the TAU link because the photon-collection capabilities of the small navigational telescope are limited. With a two-telescope system, however, a detection-sensitivity gain of several decibels can be achieved by specific tailoring of the large telescope for communications. It is concluded that for most planetary missions, adopting a two-telescope system, which may raise the system cost by about two percent, can substantially improve system performance.

Acknowledgment

The author wishes to thank James R. Lesh for his useful comments and helpful suggestions.

References

[1] E. L. Kerr, "Strawman Optical Reception Development Antenna (SORDA)," *TDA Progress Report 42-93*, vol. January–March 1988, Jet Propulsion Laboratory, Pasadena, California, pp. 97–110, May 15, 1988.

[2] E. L. Kerr, "An Integral Sunshade for Optical Reception Antennas," *TDA Progress Report 42-95*, vol. July–September 1988, Jet Propulsion Laboratory, Pasadena, California, pp. 180–195, November 15, 1988.

[3] E. L. Kerr, "Architectural Design of a Ground-based Deep-space Optical Reception Antenna," submitted for publication in *Opt. Eng.*

[4] W. K. Marshall and B. D. Burk, "Received Optical Power Calculations for Optical Communications Link Performance Analysis," *TDA Progress Report 42-87*, vol. July–September 1986, Jet Propulsion Laboratory, Pasadena, California, pp. 32–40, November 15, 1986. (The program, called OPTI or *Optical Communications Link Analysis Program*, program number NPO 17444, is available from COSMIC, 382 East Broad Street, University of Georgia, Athens, GA 30602.)

[5] I. R. King, "Accuracy of Measurement of Star Images on a Pixel Array," *Publications Astron. Soc. Pacific*, vol. 95, no. 564, San Francisco, California, pp. 163–168, February 1983.

[6] S. Faber, "The Optimum Match Between Image Size and the Size of Detector Pixels: The Choice of Angular Scale," *Keck Observatory Report No. 61*, University of California, Berkeley, Lawrence Berkeley Laboratory, June 1981.

[7] J. Nelson, T. Mast, and S. Faber, "The Design of the Keck Observatory and Telescope (Ten-Meter Telescope)," *Keck Observatory Report No. 90*, University of California, Berkeley, Lawrence Berkeley Laboratory, January 1985.

Table 1. Optical communication link parameters

Parameter name	Value[a]			
	A	B	C	D
Transmitter characteristics:				
Aperture diameter, m	0.05	0.3	0.3	1.0
Central obscuration diameter, m	0	0.06	0.06	0.2
Optics efficiency	0.65	0.65	0.65	0.65
Beam width, μrad	15	3	3	0.55
Root-mean-square pointing bias error, μrad	1.5	0.3	0.3	0.05
Root-mean-square pointing jitter, μrad	1.5	0.3	0.3	0.05
Average laser output power, W	0.1	2	2	10
Laser wavelength, nm	850	532	532	532
Laser pulse-width, ns	10	10	10	10
Channel characteristics:				
Earth atmosphere transmission	0.5	0.5	0.5	0.5
Range, astronomical units	0.0026	1.5	10.5	$\leq$1000
Daytime typical sky background radiance, $W/(m^2 \cdot sr \cdot nm)$	0.2	0.2	0.2	0.2
Nighttime typical sky background radiance,[b] $10^{-8} W/(m^2 \cdot sr \cdot nm)$	0.476	0.476	0.476	0.476
1-meter telescope characteristics:				
Aperture diameter, m	1	1	1	1
Central obscuration diameter, m	0.3	0.3	0.3	0.3
Nominal HWHM image radius for a point source, μrad	3	3	3	3
Optics efficiency	0.4	0.4	0.4	0.4
Detector quantum efficiency	0.5	0.5	0.5	0.5
Filter bandwidth for spacecraft tracking, nm	0.1	0.1	0.1	0.1
Filter bandwidth for navigational startracking, nm	200	200	200	200
10-meter telescope characteristics:				
Aperture diameter, m	10	10	10	10
Equivalent obscuration diameter, m	4.3	4.3	4.3	4.3
Nominal HWHM image radius for a point source, μrad	100	100	100	100
Optics efficiency	0.4	0.4	0.4	0.4
Detector quantum efficiency	0.5	0.5	0.5	0.5
Filter bandwidth for spacecraft tracking, nm	0.1	0.1	0.1	0.1
Filter bandwidth for navigational star tracking, nm	200	200	200	200

[a] The letters A, B, C, and D represent Moon-Earth, Mars-Earth, Saturn-Earth, and the Thousand Astronomical Unit (TAU) communication link, respectively.

[b] The nighttime sky background radiance given here corresponds to a star of visual magnitude 21.25 per arcsec^2 area in the sky.

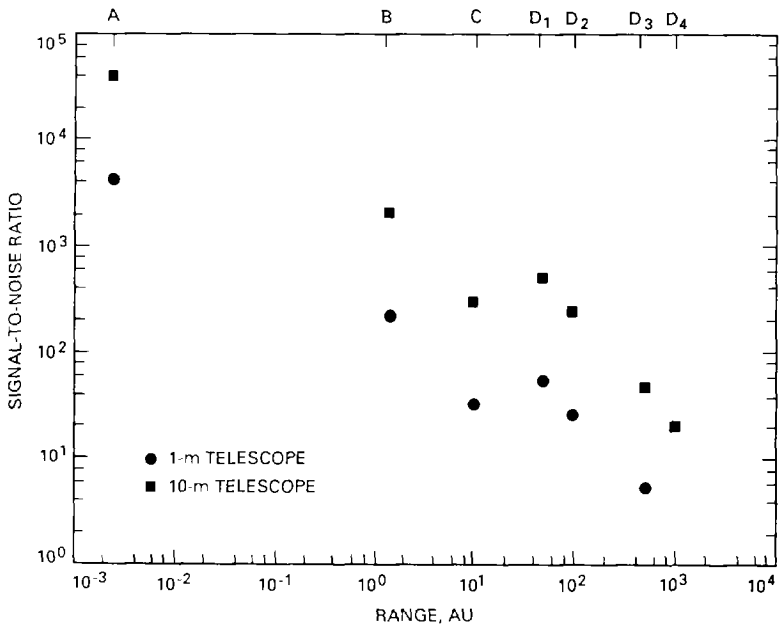

Fig. 1. Nighttime SNR with a 50-msec integration time for 1-m and 10-m telescopes, which are compared for various communication links (telescope characteristics are given in Table 1).

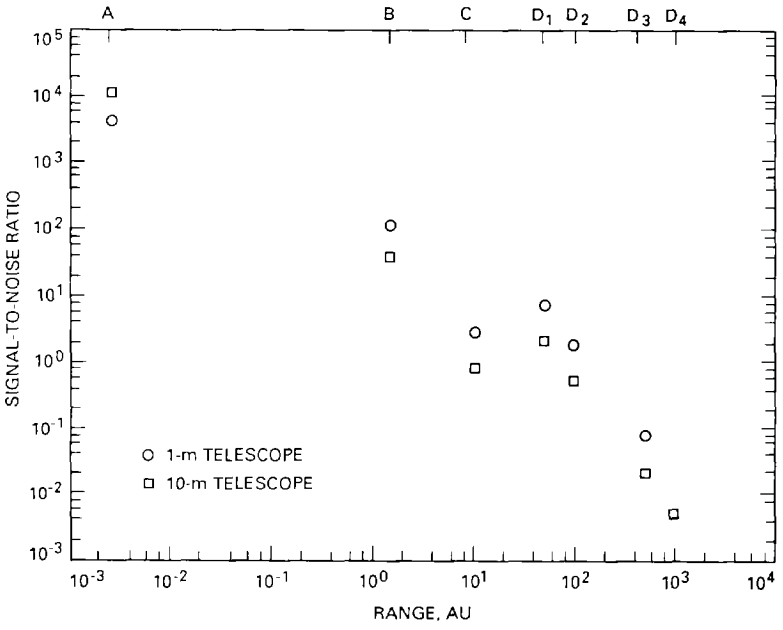

Fig. 2. Daytime SNR with a 50-msec integration time for 1-m and 10-m telescopes, which are compared for various communication links (telescope characteristics are given in Table 1).